How Fast is a Finite Gas Transient Wave and Why Does it Steepen?

ASME PVP, July 2023 Atlanta, Georgia USA

AUTHOR

Trey Walters, PE
Applied Flow Technology
Colorado Springs, CO USA

Scott Lang, PE
Applied Flow Technology
Colorado Springs, CO USA

AFT
Applied Flow Technology

Proceedings of the ASME 2023
Pressure Vessels & Piping Conference
PVP2023
July 16-21, 2023, Atlanta, Georgia, USA

PVP2023-108499

HOW FAST IS A FINITE GAS TRANSIENT WAVE AND WHY DOES IT STEEPEN?

Trey Walters, PE[1] and Scott Lang, PE[1]

[1]Applied Flow Technology, Colorado Springs, CO

ABSTRACT

Solving the transient compressible flow equations is hard. To help engineers make everyday decisions, simplified methods have been developed. One such simplification is used in the estimation of transient forces in steam pipe systems. An incomplete understanding related to gas wave speed has resulted in a method which does not reliably give conservative pipe force estimates, potentially resulting in unsafe designs. This paper develops gas wave speed predictions from first principles for compression waves moving into a non-zero steady-state flow. It is shown how the length of a family of waves steepens more quickly than previously thought. Implications for transient pipe force estimation are discussed.

KEYWORDS:

Steam hammer, piping loads, transient simulation, transient compressible flow

NOMENCLATURE

Variables and symbols

a	wave speed (ft/s / m/s)
A	cross-sectional area (ft^2 / m^2)
c	acoustic (sonic) velocity (ft/s / m/s)
c_p	specific heat at constant pressure (Btu/lbm-R / kJ/kg-K)
D	diameter (ft / m)
f	friction factor, Darcy-Weisbach (-)
F	force (lbf / kN)
$\mathbb{F}$	Aggregated parameter in Eq. 25 (units as in Eq. 25)
h	static enthalpy (Btu/lbm / kJ/kg)
h_o	stagnation enthalpy ($h + V^2/2$) (Btu/lbm / kJ/kg)
g	gravitational acceleration (32.2 ft/ s^2 / 9.81 m/s^2)
L	length (ft / m)
P	static pressure (psi / kPa)
$\dot{Q}$	heat rate (Btu/hr / kW)
t	time (sec)
$t = 0^+$	time increment just after valve starts to close (sec)
t_c	closing time of a valve (sec)
V	fluid velocity (ft/s / m/s)
x	axial distance (ft / m)
β	coefficient of volume expansion (1/R / 1/K)
γ	isentropic expansion coefficient (-)
ρ	static density (lbm/ft^3 / kg/m^3)
Θ	pipe slope angle (degrees)

Subscripts

b	back (of wave family)
f	front (of wave family)
J	Joukowsky Eq.
M	minus (direction in pipe)
P	plus or positive (direction in pipe)
SS	steady-state

1. INTRODUCTION

The topic of transient compressible flow has many important applications in industry. Among these are the prediction of:

- pipe forces in high pressure steam piping in nuclear and fossil power stations during shut down events
- the rate of pressure change in gas turbine supply conditions during system transients in order to avoid unplanned shut downs
- the disruption of flow conditions to air and gas compressors to avoid unplanned shut downs
- pipe forces during pressure relief events
- pipe flow during tank blowdown and charging events

The complications of accurately simulating such behavior have been noted by many authors over many decades (Safwat, 1978 (1), Thorley and Tiley, 1987 (2), Vardy and Pan, 2000 (3)). As a result, it is often the case that simplified calculation methods have been adopted to assist engineers in making practical design decisions. However, when evaluating finite magnitude and finite length waves, the authors note frequent misconceptions in published methodologies. Some of these misconceptions can

result in significantly unconservative predictions used for design purposes.

The purpose of this paper is to untangle some of these misconceptions as they relate to wave speed in steam and gas piping. More specifically, it is typical in industrial systems that waves have a finite magnitude (they cannot be accurately treated with infinitesimal wave methodology) and, perhaps more importantly, they have a finite length (as part of a wave family, discussed below). In other words, they are not instantaneous. They have a starting time (e.g., when a valve begins to close) and an ending time (e.g., when the valve finally closes). As is commonly known, this finite process over time generates a family of waves. The family of waves results when, during each infinitesimal increment of time, the valve position changes slightly thereby generating a new incremental wave. Over the entire valve closure time numerous incremental waves are generated. These waves are referred to here as a wave family. The length of this family of waves can change with time. Why? Because the wave speed at the front of the wave family is not the same as the wave speed at the back.

Properly understanding why this length changes over time leads to a better understanding of how fast a family of compression waves can steepen (i.e., the back of the wave family catching up with the front). This has immensely important applications in predicting forces (e.g., on pipe sections bounded by direction changes such as elbows). If a wave can steepen more quickly, it can exert a greater imbalanced force when it passes through a given pipe section.

In order to better understand why wave steepening is important, we will first give a summary of calculating transient pipe forces in gas systems. Second, an analytic solution of compressible gas flow will be reviewed for the case of perfect gases in frictionless, adiabatic pipe flow. Fortunately, the analytical solution will help us clearly determine gas wave speed and see how and why wave steepening happens. Third, simulation results of compressible flow of real gases with friction included will be discussed. This will be compared and contrasted to analytic solutions to better understand the wave steepening effect in industrial systems.

2. ESTIMATING TRANSIENT FORCES IN GAS PIPING RUNS

2.1 Background and history

The estimation of forces in piping runs involves the rigorous application of Newton's Second Law of Motion to the pipe structure. The acting forces on a pipe control volume are those from the transient fluid motion. Transient compressible flow solutions are difficult to obtain, especially on real world systems with real gas behavior and friction. This means that applying Newton's Second Law to determine transient forces on a pipe control volume is often complicated by the lack of a reliable flow solution.

To make this conundrum as simple as possible to grasp, consider trying to apply Newton's $F = ma$ when one does not know the mass, m, or the acceleration, a. One has to know these in order to apply Newton.

In a large majority of gas systems the relatively low gas density (as compared to liquids) means that transient pipe forces are quite small or even negligible. In such cases, there is no need to deal with the complexity of estimating forces from Newton's Second Law. However, there are some applications where the transient forces are not negligible, and engineers must deal with the complexity somehow so they can ensure their gas system designs are safe. One such application is steam hammer in power station piping.

In the 1980s two papers were written that provide a foundation for how to estimate transient forces. The first paper by Lee and Goodling, 1982 (4) explains that, by the early 1980s, hard experience in modern power stations was teaching engineers that they needed to take more seriously the ability of transient forces in steam systems to cause significant damage to piping and pipe structural supports. Their paper gives a proper explanation of applying Newton's Second Law to estimating pipe forces due to steam transient effects. They also appear to be the first to introduce a simplifying method of force estimation based on the Joukowsky equation and valve closure times.

A few years later a second paper was written (Goodling, 1989 (5)) that explicitly laid out a step-by-step methodology for the simplified transient force estimation introduced in Lee and Goodling, 1982 (4). These two papers make up what is today known to engineers around the world as "the Goodling Method". One can see how this method has become standard engineering practice in other papers such as Stakenborghs and Dziuba, 2009 (6) and Moody and Stakenborghs, 2018 (7). It is commonly accepted that the Goodling Method provides conservatively high transient force profiles.

One important assumption in the Goodling Method is that wave steepening is negligible in pipe runs of length typically seen in steam power station applications. Recent years have seen a questioning of this assumption and in general a questioning of whether the Goodling Method is in fact conservative (Rovagnati and Gray, 2014 (8), Rovagnati and Gray, 2015 (9), Mayes, Gawande and Williams, 2017 (10) and Mayes and Gawande, 2018 (11)). These four papers observed the wave steepening effects in simulations based on the Method of Characteristics (MOC) (8-9) and using a finite-difference based CFD tool (10-11). The wave steepening effect was observed in pipe run lengths that may be found in power station steam systems. This was observed by different authors using different tools with different transient equation solution techniques – which lends at least some credence to the claims. However, no underlying reasons based on physics or theory were given by these authors for this wave steepening. As a result, when Moody and Stakenborghs, 2018 (7) gave a physics-based reason why the wave steepening effect presented by the other authors could not be as significant as claimed, the matter seemed to have been put to rest.

Our contention in this paper is that there is more to the story on wave steepening and we offer a physics-based reason which supports the conclusions in the four papers [8-11] which question Goodling. We argue that the physics-based explanation of

Moody and Stakenborghs, 2018 (7) overlooks critical details and is not valid. As noted in our Introduction, this is significant because it means that standard engineering practice for estimating transient pipe forces may not be conservative – potentially leading to unsafe designs in existing fossil and nuclear power stations currently in operation.

2.2 Summary of transient pipe force calculation for instantaneous compression event

Unfortunately, there is not enough space in this paper to offer a thorough explanation of transient forces in gas piping. As noted earlier, the discussion of Newton's Second Law applied to transient steam flow outlined by Lee and Goodling 1982 (4) was sound. The authors explore this in detail in Lang and Walters, 2022 (12). A brief summary will be given here before moving on to the reasons why waves steepen more quickly than previously thought.

Consider a system we all have experience with – a garden hose. When steady flow through the hose is established, and the hose is restrained at each endpoint (by the supply nozzle at one end and a human hand at the other), the hose does not move. It is in equilibrium because all forces add to zero. Forces do exist (pressure, friction, gravity, etc.) but they all negate each other.

However, when a transient is introduced (e.g., a human hand suddenly closes off the flow at the discharge) the hose will often move. This movement is due to temporary imbalanced forces caused by waterhammer. Once a new steady-state is established, the equilibrium in forces once again occurs and the hose stops moving.

When discussion is given in this paper on transient force calculation, it is focused completely on this short duration imbalance which exerts forces on the hose (or pipe) causing it to move if not properly supported. If the hose/pipe supports are placed in the proper location with proper strength, the hose/pipe will not move. But in order to prevent the movement, the supports must take the loads which are generated by the transient. Steam hammer and gas transients work in a generally similar manner.

Consider Fig. 1. For simplicity, assume the gas flow is frictionless and adiabatic and the pipe is horizontal. This means the initial, steady-state (*SS*) conditions are uniform everywhere in the pipe. As such, the pressure and velocity everywhere are P_{SS} and V_{SS}. A valve is closed instantly somewhere downstream, generating a single compression wave which moves from right to left at wave speed $a_M = V_{SS} - c_{SS}$. The wave front will pass through the pipe run referred to as Leg 1-2. Fig. 1 shows a snapshot of time with the wave passing through this pipe leg. This pipe leg has 90-degree elbows at each end point labeled as 1 and 2. The gas behind the wave front (at the right) has an increased pressure shown in the red shaded area in Fig. 1, and the pressure is P_{high}.

The dominant transient forces in this example will be the pressure forces acting on the projected cross-sectional area in the x direction of pipe Leg 1-2. We will call this area $A_{(\mathrm{L},1\text{-}2)x}$. The projected area equals the cross-sectional area of Leg 1-2.

Neglecting other terms in Newton's Second Law for simplicity yields the instantaneous force of the fluid on the pipe in the x direction as

$$F_x \approx P_2 A_{(\mathrm{L},1\text{-}2)x} - P_1\left(A_{(\mathrm{L},1\text{-}2)x}\right)$$

Or, more simply,

$$F_x \approx (P_2 - P_1) A_{(\mathrm{L},1\text{-}2)x} \qquad (1)$$

Because the pressure at P_2 is the higher pressure and equal to P_{high}, the fluid force at location 2 is higher than at location 1. The net force acts on the pipe in the positive x direction, pushing the pipe Leg 1-2 to the right. This transient force will last until the wave front has moved past location 1. After that, the transient force, F_x, will return to zero as the pressures at locations 1 and 2 will be the same.

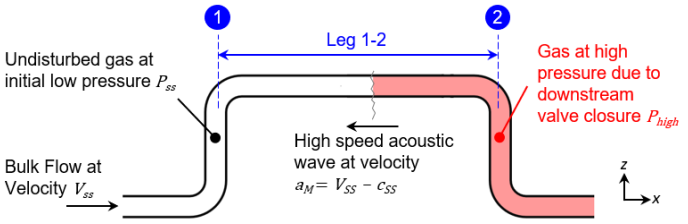

FIGURE 1: PIPE SCHEMATIC WITH ELBOW PAIR AT LOCATIONS 1 AND 2 SHOWING PRESSURE WAVE MOVING FROM RIGHT TO LEFT AT WAVE SPEED a_M

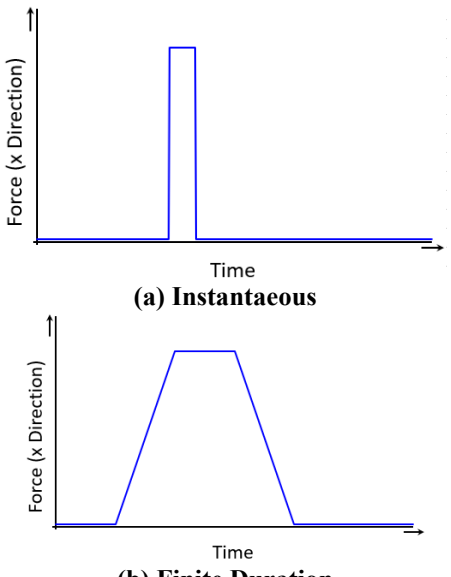

FIGURE 2: TRANSIENT FORCE IN PIPE LEG 1-2 FROM (A) AN INSTANTANEOUS COMPRESSION WAVE AND (B) A FINITE DURATION (NON-INSTANTANEOUS) WAVE

The force over time will simply be a square wave as shown in Fig. 2a. The maximum force is determined from Eq. 1. The duration of the non-zero force in Fig. 2a is just the length of pipe, $L_{(L,1\text{-}2)}$, divided by the wave speed absolute value, a_M:

$$\Delta t = \frac{L_{(L,1\text{-}2)}}{|a_M|}$$

2.3 Summary of transient pipe force calculation for finite duration compression event

Transient events in real systems are never instantaneous. What this means is that a valve which closes over some finite time generates a family of compression waves upstream of the valve. Depending on the length of time to close the valve and the length of the pipe leg, a transient force profile will usually look more like that in Fig. 2b. Here the maximum force is less than calculated in Eq. 1 because the length of the wave family generated during the finite valve closure time is longer than the pipe leg length. Hence, the pipe leg never experiences the full pressure difference as shown in Eq. 1 and Fig 1. If wave steepening is negligible, then all pipe legs of equal length bounded by elbows will have the profile as in Fig. 2b regardless of where they are located along the pipe length. For more on this see Goodling, 1989 (5).

3. TRANSIENT GAS FLOW SIMPLE ANALYTICAL SOLUTION

3.1 Fundamental equations

Before considering the flow of real gases with friction, some key insights can be obtained by considering frictionless, adiabatic flow of a calorically perfect gas in a constant diameter, horizontal pipe. Anderson, 2004, Section 7.6 (13) offers a clear development of the flow equations.

From Mass, Momentum, and Energy Conservation, Eqs. 2 and 3 can be derived:

$$\frac{\partial P}{\partial t} + V\frac{\partial P}{\partial x} + \rho c^2 \frac{\partial V}{\partial x} = 0 \tag{2}$$

$$\frac{\partial V}{\partial t} + V\frac{\partial V}{\partial x} + \frac{1}{\rho}\frac{\partial P}{\partial x} = 0 \tag{3}$$

Sonic velocity symbols in gas dynamic literature are conventionally referred to as either c or a. Here we will use c and reserve the symbol a for gas wave speed. The velocity, V, is relative to the pipe axial coordinate direction, x, and can be positive or negative. On the other hand, the sonic velocity, c, is a thermodynamic parameter and always positive with no directional qualities.

To make the differences more clear we will add a subscript to a – typically a_P or a_M for the wave speed in the plus and minus axial x-coordinate direction. As a result, a_P will always be positive and a_M will always be negative for subsonic flows.

While this is potentially confusing to those accustomed to using a to represent sonic velocity in gases, this offers the advantage of having common symbology for wave speed with that conventionally used in liquid waterhammer theory. Note also that in liquid waterhammer theory, it is commonly assumed that $|a| >> |V|$ and thus V can be ignored when determining liquid wave speed. In other words, a is the same absolute value in the plus and minus directions for liquids. In this paper the terms gas "wave velocity" and gas "wave speed" will be used interchangeably.

Eqs. 2 and 3 can be combined and solved along positive and negative characteristic lines such that:

$$dP \pm \rho c dV = 0 \tag{4}$$

along a line of constant $V + c$ for the positive value in Eq. 4 and $V - c$ for the negative value.

Using the definition of sonic velocity and basic isentropic relationships Anderson shows that the following is true for the C^+ characteristic:

$$V + \frac{2c}{\gamma - 1} = \text{Const1} \tag{5}$$

and for the C^- characteristic:

$$V - \frac{2c}{\gamma - 1} = \text{Const2} \tag{6}$$

where γ is the isentropic expansion coefficient.

These two constants, Const1 and Const2, are Riemann invariants.

3.2 Application to a finite duration compression wave

Consider the pipe in Fig. 3 with length, L, and diameter, D. The pipe is frictionless, horizontal and adiabatic and thus the initial, steady-state (SS) conditions in the pipe are uniform everywhere. At time zero a valve begins to close at point 2. The velocity at the exit, point 2, is reduced linearly from V_{SS} to zero over some time, t_c , as shown in Fig. 4. The pressure and temperature at point 1 are maintained constant.

FIGURE 3: FRICTIONLESS, HORIZONTAL PIPE WITH INITIAL FLOW FROM LEFT TO RIGHT.

As soon as the valve starts to close (at $t = 0^+$) the first compression wave is generated and starts moving to the left at a *wave* velocity, a_M, of:

$$a_{M,t=0^+} = V_{SS} - c_{SS} \tag{7}$$

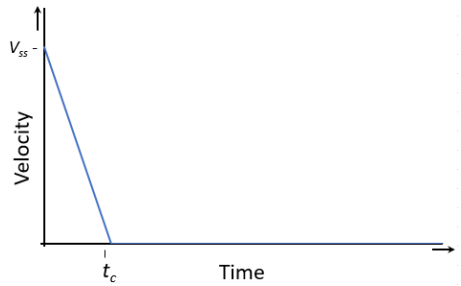

FIGURE 4: VELOCITY REDUCTION PROFILE IN FIG. 3 PIPE AT EXIT POINT 2

The wave speed in Eq. 7 is that at the front of the wave family. As the velocity is continuously reduced at the valve, each increment of time will generate another compression wave into the disturbed flow field behind the preceding waves. When the valve finishes closing then the final wave of the wave family will be generated and travel to the left at a wave speed of:

$$a_{M,t=t_c} = V_{t_c} - c_{t_c} \tag{8}$$

But V at t_c is zero because the valve is closed, so Eq. 8 becomes:

$$a_{M,t=t_c} = -c_{t_c} \tag{9}$$

The question then becomes, what is c_{tc} in Eq. 9? If it is greater in magnitude than the wave speed at the front in Eq. 7, the wave family will steepen and the back of the wave family will eventually catch up with the front if the pipe is long enough.

We can solve for Const1 in Eq. 5 using the known and spatially uniform steady-state conditions:

$$V_{SS} + \frac{2c_{SS}}{\gamma-1} = \text{Const1} \tag{10}$$

Since Const1 is Riemann invariant, we can use that to solve for c_{tc} knowing that the velocity, V, is zero at point 2 at time t_c.

$$\frac{2c_{tc}}{\gamma-1} = \text{Const1} \tag{11}$$

Equating Eqs. 10 and 11 allows us to obtain the sonic velocity and (from Eq. 9) the wave speed at the back of the wave family:

$$c_{t_c} = c_{SS} + \frac{\gamma-1}{2}V_{SS} \tag{12}$$

To make the difference in the front and back of the wave family clearer, we will introduce the subscripts f and b for the front and back of the wave family:

$$a_f = a_{M,t=0^+}$$
$$a_b = a_{M,t=t_c}$$

Using Eqs. 7, 9 and 12 we can now determine the wave speed at the back of the wave family based on steady-state conditions only:

$$a_b = a_f - V_{SS}\left(\frac{\gamma+1}{2}\right) \tag{13}$$

At first glance Eq. 13 seems to be saying that a_b is less than a_f and, hence, the back of the wave will travel more slowly than the front. However, remember that a_b and a_f have directions. And they travel in the *opposite direction* of the steady-state velocity, V_{SS}. In other words, a_f and a_b are *negative* values, so the back of the wave family travels *faster* in the negative x-direction than the front by the absolute value of $V_{SS}\left(\frac{\gamma+1}{2}\right)$. This, therefore, is the speed at which the wave will steepen. To make this clearer going forward, we will introduce a new parameter, Δa_{fb}:

$$\Delta a_{fb} = V_{SS}\left(\frac{\gamma+1}{2}\right) \tag{14}$$

An equivalent way of determining Δa_{fb} is to subtract Eq. 7 from 9. The advantage of Eq. 14 is that it is based entirely on initial conditions.

$$\Delta a_{fb} = c_b - c_{SS} + V_{SS} \tag{15}$$

Given enough pipe length and time, the back of the wave will catch up with the front and form a shock wave. We will call this time t_{shock} and the length needed to reach this point L_{shock}. Measuring L_{shock} as the distance from point 2 (in Fig. 3) it is easily observed that:

$$L_{shock} = |a_f| t_{shock}$$

and

$$L_{shock} = |a_b|(t_{shock} - t_c)$$

Equating these and using Eqs. 7, 9 and 12, one can solve for t_{shock} entirely in terms of the initial conditions in the pipe. Then L_{shock} follows from either of the preceding equations. The result is:

$$t_{shock} = \left(1 + \left(\frac{2}{\gamma+1}\right)\left(\frac{c_{SS}}{V_{SS}} - 1\right)\right)t_c \tag{16}$$

$$L_{shock} = (c_{SS} - V_{SS})\left(1 + \left(\frac{2}{\gamma+1}\right)\left(\frac{c_{SS}}{V_{SS}} - 1\right)\right)t_c \tag{17}$$

While we have not discussed pressure here in Section 3, it can be shown that the pressure at the back of the wave family is given by the following (Anderson (13), Eq. 7.86 or Moody (14), Eq. 8.10):

$$P_b = P_{SS}\left(1 + \left(\frac{\gamma-1}{2}\right)\left(\frac{V_{SS}}{c_{SS}}\right)\right)^{2\gamma/(\gamma-1)} \quad (18)$$

3.3 Example 1

Consider a numerical example following from the previous equations. Assume a horizontal, constant diameter pipe as in Fig. 3 with frictionless, adiabatic flow of a calorically perfect gas. A valve closes at point 2 with a linear velocity profile as in Fig. 4. This will generate a family of compression waves that travel from the right to left in Fig. 3. The tables below show the inputs and calculated values.

Inputs:

Length (L)	1000 m
Steady-State velocity (V_{SS})	41.77 m/s
Steady-State sonic velocity (c_{SS})	567.0 m/s
Steady-State pressure (P_{SS})	7000 kPa
γ	1.4
Closing time (t_c)	0.1 sec

Calculated Values:

Parameter	Eq.	Value
Wave speed front of wave family $\|a_f\|$	7	525.24 m/s
Wave speed back of wave family $\|a_b\|$	13	575.36 m/s
Speed at which back catches front (Δa_{fb})	14	50.12 m/s
Sonic velocity back of wave family (c_b)	12	575.36 m/s
Time for back to catch front (t_{shock})	16	1.148 sec
Length where back catches front (L_{shock})	17	602.9 m
Pressure at back of wave family (P_b)	18	7754.6 kPa

Using these values Fig. 5 can be assembled. Here one can see the path of the front of the wave family as the lower curve, the path of the back of the wave family as the upper curve, with both traveling from right to left. Fig. 5 shows how at any given time the back of the wave family is catching up with the front. Also noted in Fig. 5 is t_{shock} at 1.148 s, and the shock location $x_{shock} = L - L_{shock}$ which is 397.1 m.

Several Regions are noted in Fig. 5.

- Region 1: This entire region represents the initial, steady conditions.
- Region 2: This is the region inside the wave family where conditions continuously vary with x and t. It is possible to determine analytical relationships for all parameters in Region 2 but these are not shown here as they are not needed to support the present study. This area is where the family of waves exist.
- Region 3: This entire region represents the conditions after the back of the wave family has passed.

With Example 1 in place, let's consider what happens to transient forces inside the pipe. If the pipe is straight for the entire length and restrained at the ends, no transient forces will be generated that require additional pipe restraints. But what if the pipe is not straight at all points?

Assume in the Fig. 3 pipe that there are three closely spaced elbow pairs in the x-direction like that shown in Fig. 1, perhaps needed for the pipe to cross over roads or for mitigating thermal expansion of the pipe. Each elbow pair has the same geometry in that the vertical rise in the z-direction is the same and the x-distance between the elbows at the top is the same (specified as 5 m). Finally, assume these elbow pairs are spaced starting from the right at a linear pipe length of 50 m, 300 m and 550 m. In other words, the x location of each elbow pair in Fig. 3 is at 950 m, 700 m and 450 m. Table 1 shows the data for the elbow pair locations. Finally, assume the pipe diameter, D, is 1 m.

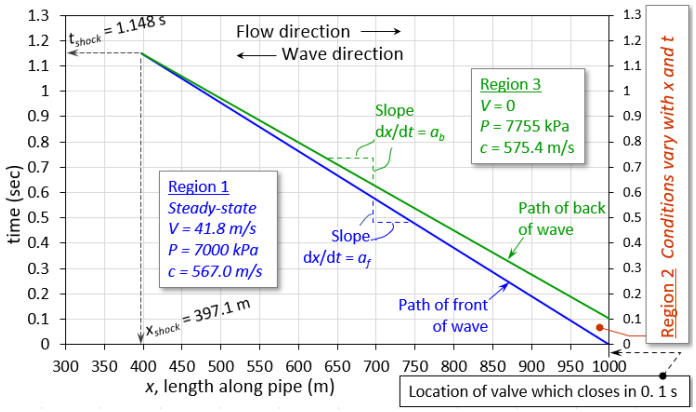

FIGURE 5: PATHS OF FRONT AND BACK OF WAVE FAMILY (FROM RIGHT TO LEFT) IN EXAMPLE 1

TABLE 1: LOCATION OF ELEVATED ELBOW PAIRS IN EXAMPLE 1

Elbow Pair ID	Distance from Valve (m)	x (m)
Leg 1-2	50	950
Leg 3-4	300	700
Leg 5-6	550	450

The pressure profile when the front of the wave reaches the upstream side of each elbow pair is shown in Fig. 6. Fig. 6 clearly shows how the wave steepens as it progresses to the three elbow pair locations at 950, 700 and 450 m.

The bottom graph in Fig. 6 shows a blow up of the top graph at each of the elbow locations. Also shown are the pressure differences that will drive the transient forces using Eq. 1. It is clear that the pressure differences, and hence forces, increase significantly as the wave moves to the left and steepens.

As discussed earlier, a more accurate determination of the forces in Fig. 6 would consider all terms in Newton's Second Law (12). In pipe runs of straight pipe with no diameter changes

or fittings between elbow pairs (such as in the present example) Eq. 1 offers a quick approximation to the forces.

Using Eq. 1 on the Fig. 6 results obtains the forces shown in Table 2.

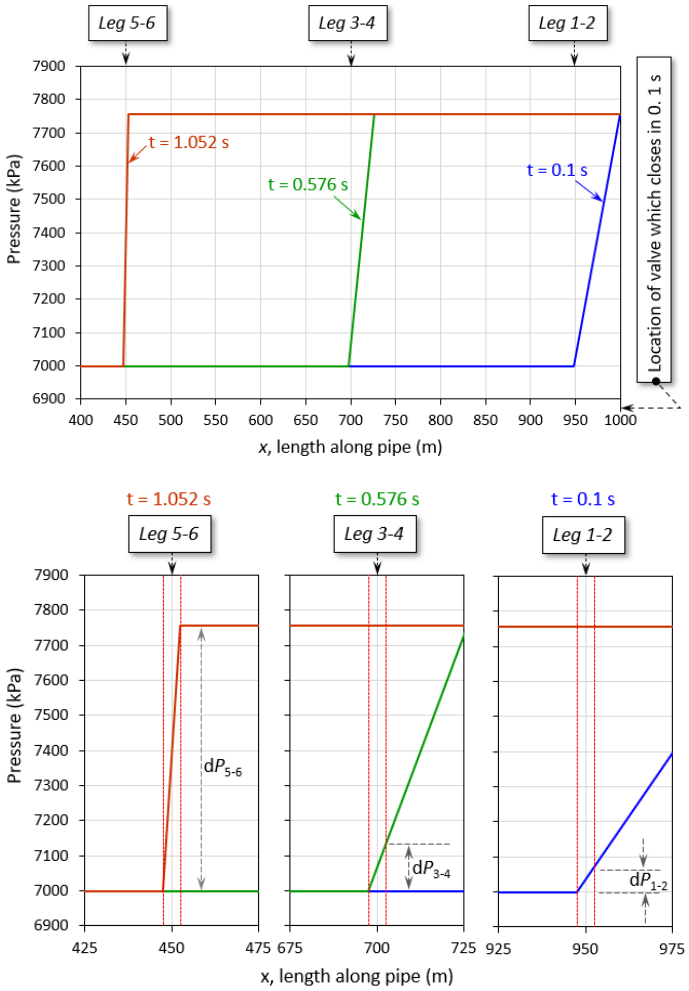

FIGURE 6: PRESSURE PROFILES AT THREE POINTS IN TIME FOR EXAMPLE 1 SHOWS WAVE STEEPENING. TOP SHOWS PROFILES AS THEY PROGRESS IN TIME RIGHT TO LEFT. BOTTOM SHOWS BLOW UP PROFILES WITH THE ELBOW LOCATIONS ALSO SHOWN AS VERTICAL LINES. RESULTS DETERMINED USING SIMPLIFIED ANALYTICAL SOLUTION.

TABLE 2: APPROXIMATE MAXIMUM TRANSIENT FORCES IN EXAMPLE 1

Elbow Pair ID	Distance from Valve (m)	*dP* (kPa/psid)	*F ≈ dP*A* (kN/lbf)
Leg 1-2	50	67 / 10	54 / 12100
Leg 3-4	300	126 / 18	100 / 22500
Leg 5-6	550	755 / 110	593 / 133000

Note that Goodling's Method (calculations not shown here for brevity) would yield 52.5 kN (11800 lbf) for all three of the pipe run legs in Table 2. It is roughly correct for Leg 1-2, but far underpredicts Leg 3-4 and Leg 5-6.

One observation here is that the Goodling Method is likely to be approximately accurate for elbow pairs near the source of the transient and before significant wave steepening has happened. As the wave travels further from the transient Goodling will become less accurate. This is consistent with findings by Rovagnati and Gray, 2015 (9).

Another interesting observation is that the impact of compressible flow is often assumed to be of low significance at lower Mach numbers. In this example the highest Mach number is 0.08. But one can see a significant impact on results. This should be a cautionary tale for engineers who are quick to dismiss low Mach number gas flow applications as having negligible compressibility effects.

4. SOLVING COMPLETE TRANSIENT GAS FLOW EQUATIONS

Including real gas behavior, friction, gravity effects and heat transfer in transient compressible flow significantly complicates the solution process and closed form analytical solutions are no longer possible. But it offers more realistic results.

Moody, 1990 (14) offers a formulation of the complete fundamental equations that lends itself to an MOC solution – albeit with grid interpolations required as is typical in gas transients (1-3). Moody's formulation allows for pipe geometry changes (non-constant diameter in space and/or time) as well as axial heat conduction in the gas. These two elements are not considered here leaving us with Moody's formulation as follows:

From Mass Conservation:

$$\frac{\partial \rho}{\partial t} + V\frac{\partial \rho}{\partial x} + \rho\frac{\partial V}{\partial x} = 0 \tag{19}$$

From Momentum Conservation:

$$\frac{\partial V}{\partial t} + V\frac{\partial V}{\partial x} + \frac{1}{\rho}\frac{\partial P}{\partial x} + \frac{f\,V\,|V|}{2D} + g\sin(\theta) = 0 \tag{20}$$

From Energy Conservation:

$$\frac{\partial h_o}{\partial t} + V\frac{\partial (h_o + gz)}{\partial x} - \frac{1}{\rho}\frac{\partial P}{\partial t} - \frac{1}{\rho A}\frac{\dot{Q}}{\partial x} = 0 \tag{21}$$

The MOC ODE transformation of Eqs. 19-21 is as follows:

Along the right running path, $\frac{dx}{dt} = V + c$:

$$\frac{dP}{dt} + \rho c\frac{dV}{dt} = \frac{\beta c^2}{c_p}\mathbb{F} - \rho c\left[g\sin\theta + \frac{f\,V\,|V|}{2D}\right] \tag{22}$$

Along the left running path, $\frac{dx}{dt} = V + c$:

$$\frac{dP}{dt} - \rho c \frac{dV}{dt} = \frac{\beta c^2}{c_p} \mathbb{F} + \rho c \left[g \sin\theta + \frac{f\, V\, |V|}{2D} \right] \quad (23)$$

Along the particle path, $\frac{dx}{dt} = V$:

$$\frac{dP}{dt} - c^2 \frac{d\rho}{dt} = \frac{\beta c^2}{c_p} \mathbb{F} \quad (24)$$

Where:

$$\mathbb{F} = \frac{f \rho |V^3|}{2D} + \frac{\dot{Q}}{A\, dx} \quad (25)$$

Moody (14) then gives a convenient organization of three compatibility equations and a recommended interpolation scheme to solve Eqs. 22-24. An implementation of Moody's method (15) will be used here to compare the simplified analysis in Section 3 to a more complete analysis.

4.1 Example 2

Let's use the same problem statement as in Example 1 but now include friction and real gas modelling. We assume the gas is air in the model. The boundary condition at point 2 in Fig. 3 is represented in the model not as a linear velocity vs. time but as a linear mass flow rate vs. time. Simulation results show that the velocity is near linear with this boundary condition. Note that the inputs are slightly different than in Example 1 because there is pressure drop in the pipe and the air is being treated as a real gas. The inputs below are from a reliable steady-state solution (15) at the pipe endpoint (location 2).

Inputs and Initial Values:

Length (L)	1000 m
Diameter (D)	1 m
Steady-State mass flow rate	1000 kg/s
Steady-State inlet/outlet velocity (V_{SS})	42.76 / 44.61 m/s
Steady-State inlet/outlet pressure (P_{SS})	7000 / 6702 kPa
Steady-State inlet/outlet temperature	526.8 / 526.9 C
Steady-State outlet sonic velocity (c_{SS})	572.8 m/s
γ inlet/outlet	1.399 / 1.397
Closing time (t_c)	0.1 sec

The pressure profile results are shown in Fig. 7. Table 3 shows the predicted maximum pressure differences and forces using Reference (12) – not Eq. 1. Comparing these to Example 1 (Fig. 6 and Table 2) one can make two observations:

1. Wave steepening occurs in a similar fashion to the frictionless, perfect gas case.
2. The forces are similar to those in Table 2 closer to the valve (Legs 1-2 and 3-4) even when including real gas modelling and friction. At the farthest elbow pair (Leg 5-6) the forces are significantly lower than Table 2.

Note that a complete application of Newton's Second Law (12) is performed in the simulation (15) to obtain the transient forces – and not just the simple Eq. 1 used in Table 2. This is why the pressure differences are higher for Legs 1-2 and 3-4 in the simulation results shown in Table 3 even though the forces are similar to Table 2.

The second observation above is impacted by several phenomena:

- Fig. 7 clearly shows line pack with the pressure at the valve (L = 1000 m) continuing to climb upward after the valve has closed. Fig. 7 shows a maximum pressure profile when the wave reaches the steam source at the left. This appears to be a maximum pressure, but after the wave reflects from the steam source the pressure continues to rise, which is not shown. However, after the first reflection the compression wave turns into an expansion wave and the wave steepening is reversed. Which means the forces are much lower than in Table 3 after reflections begin.
- The wave family at t = 0.1 seconds has not had time to steepen. So, it is not surprising the maximum transient force in Leg 1-2 is similar to Example 1 and, in fact, Goodling's Method (as noted in Section 3).
- In Example 1 the flow conditions were everywhere uniform in the pipe. Here in Example 2, there is a pressure drop due to friction and no conditions are uniform. The minimum pressure along the pipe is shown in Fig. 7 and that represents the steady-state pressure. Once the transient occurs the pressure in the pipe only increases – at least until a wave reflection occurs. What this means is that as the compression wave progresses along the pipe from right to left, the available pressure difference between the maximum and minimum envelope shrinks as seen in Fig. 7.

Putting these observations together, one can conclude that the actual forces generated in transient pipe flow with friction will have two competing effects:

1. The wave steepening which makes the transient forces *increase* the further one is away from the source of the transient.
2. The frictional pressure drop which *reduces* the potential driving pressure envelope for transient forces the further one is away from the source of the transient.

One can expect to find a location along the pipe of maximum transient force where these two competing effects combine to create an overall maximum.

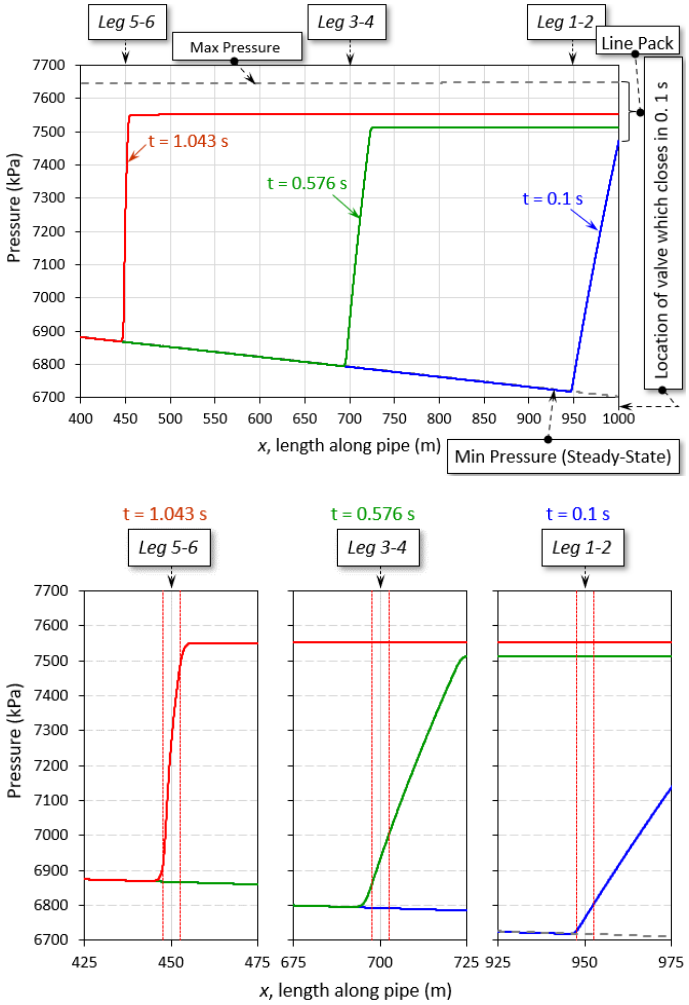

FIGURE 7: PRESSURE PROFILES AT THREE POINTS IN TIME FOR EXAMPLE 2 SHOWS WAVE STEEPENING. TOP SHOWS PROFILES AS THEY PROGRESS IN TIME RIGHT TO LEFT. BOTTOM SHOWS BLOW UP PROFILES WITH THE ELBOW LOCATIONS ALSO SHOWN AS VERTICAL LINES. MAX/MIN CURVES ARE ONLY UP UNTIL 1.85 SEC WHEN FIRST WAVE REACHES THE SOURCE. RESULTS DETERMINED USING MOC SOLUTION OF EQS. 22-24 (15).

TABLE 3: MAXIMUM TRANSIENT FORCES IN EXAMPLE 2

Elbow Pair ID	Distance from Valve (m)	*dP* (kPa/psid)	*F* (kN/lbf)	Time of Max Force (sec)
Leg 1-2	50	77 / 11	54.5 / 12300	0.103
Leg 3-4	300	144 / 21	100 / 22500	0.576
Leg 5-6	550	572 / 83	414 / 93000	1.043

5. DISCUSSION

The analysis in this paper clearly shows wave steepening, and it shows it can happen much faster and in shorter pipe lengths than previously thought – particularly in methods used in power station steam piping design. This raises questions about simplified methods like the Goodling Method. It appears this simplified method inadvertently overlooked something. What was it?

Reviewing a commentary on Goodling in Moody and Stakenborghs, 2018 (7) sheds some light on this. It appears that when considering how fast wave steepening could occur, the authors in (7) essentially used Eq. 15. But they had an oversight and neglected to consider V_{SS} in Eq. 15 and only considered the difference in sonic velocities. This resulted in Δa_{fb} estimated to be much lower than determined in our paper and lent credence to their conclusion that wave steepening was not important. Including V_{SS} in Eq. 15, or just using Eq. 14, gives a more accurate picture of how fast wave steepening occurs. However, realize that Eqs. 14 and 15 are for perfect gas, frictionless flow. When real gases and (especially) friction are included then Eq. 15 should be fairly close to the initial value of Δa_{fb}. Simulation results show that Δa_{fb} is not constant and in fact reduces with time.

Walters, 2022 (16) applies the findings presented here to steam systems and explores the Goodling Method in more depth. Other misconceptions in Goodling are discussed and direct comparisons are made to the example in Rovagnati and Gray, 2015 (9).

6. CONCLUSION

An improved understanding of gas wave speed for compression waves is offered and should be considered in future gas transient analyses. Simplified methods of estimating transient pipe forces do not consider wave steepening and may not be conservative – especially at elbow pairs further from the source of the transient. Improvements to the Goodling Method should be made by the engineering community and a review of existing steam systems designed and built using Goodling should be considered for safety reasons.

NOTE FROM THE AUTHORS

This paper has had a circuitous path to publication impacted by the COVID-19 virus. It was originally planned to precede another paper by the first author, Reference [16]. The preceding conference for the present paper was scheduled for early 2022 and thus before PVP 2022. Due to ongoing COVID-19 concerns the early 2022 conference was delayed until late 2022 – which was after Reference [16] was published. The Reference [16] analyses was based on the present paper and therefore referenced the present paper in anticipation of its publication expected in late 2022. After Reference [16] was presented in July 2022 the late 2022 conference was unexpectedly cancelled in September 2022. The present paper was therefore withdrawn from the cancelled conference and the authors sought another avenue of publication. The best option was PVP 2023. Note that Reference [16] thus has an incorrect venue reference for the present paper.

For general information, in late 2022 the cancelled conference was revived by other organizers and is now planned for April 2023.

ACKNOWLEDGEMENTS

Thanks to Ben Rovagnati and Fred Moody for their patient discussions with the first author and taking time to clarify and answer questions about their work.

REFERENCES

[1] Safwat, H. H., (1978), "Generalized application of the method of characteristics for the analysis of transients in steam lines in nuclear power plants", ASME Winter Annual Meeting, San Francisco, California, USA, December 10-15, 1978, 325-337.

[2] Thorley, A. R. D., and Tiley, C. H., (1987), "Unsteady and Transient Flow of Compressible Fluids in Pipelines – a review of theoretical and some experimental studies", International Journal of Heat and Fluid Flow, Volume 8, Issue 1, March 1987, 3-15.

[3] Vardy, A., and Pan, Z., (2000), "Numerical Accuracy in Unsteady Compressible Flows", Proc. 8th International conference on pressure surges, BHR Group, The Hague, The Netherlands, April 2000.

[4] Lee, M. Z., and Goodling, E. C., (1982), "Steamhammer in Power Plant Piping Restraint Design and Optimization", ASME Pressure Vessels and Piping Conference, Orlando, Florida, USA, Vol. 69, June 27, 1982.

[5] Goodling, E. C., (1989), "Simplified Analysis of Steam Hammer Pipe Support Loads", ASME/JSME Pressure Vessels and Piping Conference, Honolulu, Hawaii, USA, July 23-27, 1989, PVP Vol 165.

[6] Stakenborghs, R., and Dziuba, L., (2009), "Simplified Approach to Establishing Bounding Main Steam Piping Support Load Increase Due to Reactor Power Uprate", 26th International Conference on Nuclear Engineering, Brussels, Belgium, July 12-16, 2009, ICONE17-75743.

[7] Moody, F. J., and Stakenborghs, R., (2018), "The Effects Of Compressibility And Piping Geometry On Steamhammer Loads", 26th International Conference on Nuclear Engineering, London, England, July 22-26, 2018, ICONE17-75743.

[8] Rovagnati, B, and Gray, J. H., (2014), "Effect of Reflection Waves on Water Hammer Loads", ASME Pressure Vessels & Piping Conference, Anaheim, California, USA, July 20-24, 2014, PVP2014-29121.

[9] Rovagnati, B, and Gray, J. H., (2015), "Fluid Compressibility Effects In Steam Hammer Analyses", ASME Pressure Vessels & Piping Conference, Boston, Massachusetts, USA, July 19-23, 2015, PVP2014-29121.

[10] Mayes, A., Gawande, K. P. and Williams, D. K., (2017), "Comparisons of CFD and Traditional Solutions For Steam Hammer Events", ASME Pressure Vessels & Piping Conference, Waikoloa, Hawaii, USA, July 16-20, 2017, PVP2017-65864.

[11] Mayes, A. and Gawande, K. P., (2018), "Effect Of Steam Hammer Pressure Wave Steepening On Pipe Supports", ASME Pressure Vessels & Piping Conference, Prague, Czech Republic, July 15-20, 2018, PVP2018-84775.

[12] Lang, S.A. and Walters, T.W. (2022), "Accurately Predicting Transient Fluid Forces in Piping Systems – Part 1: Fundamentals and Part 2: Applications", ASME Pressure Vessels & Piping Conference, Las Vegas, NV, USA, July 17-22, 2022, PVP2022- 84740 and -84748.

[13] Anderson, J. D., (2004), Modern Compressible Flow: With Historical Perspective, 3rd Edition, McGraw-Hill, International Edition, New York, New York, USA, 2004.

[14] Moody, F. J., (1990), Introduction To Unsteady Thermofluid Mechanics, Wiley-Interscience, 1990.

[15] Applied Flow Technology, (2022), *AFT xStream*, Colorado Springs, Colorado, USA.

[16] Walters, T.W. (2022), "A Critique of Steam Hammer Load Analysis Methods", ASME Pressure Vessels & Piping Conference, Las Vegas, NV, USA, July 17-22, 2022, PVP2022-83715.